J Wood Sci (2013) 59:432–441
DOI 10.1007/s10086-013-1349-z

ORIGINAL ARTICLE

Identification and species-typing of wood rotting fungi using melting curve analysis

Sakae Horisawa · Yoh Sakuma · Shuichi Doi

Received: 24 August 2012 / Accepted: 1 May 2013 / Published online: 1 June 2013

Abstract A method for identification and typing of wood rotting fungi using the melting temperature [*T*(m)] of DNA fragments coding rRNA (rDNA) was examined. The *T*(m)s of four DNA fragments, inter transcribed spacer (ITS) I, ITS II, and two partial fragments of 28S rDNA from each of 20 species of wood rotting fungi, were measured by melting curve analysis. The *T*(m) variation was large enough between species to enable identification based on the *T*(m) values. A pair of *T*(m)s of the ITS I region (between the primers ITS1 and ITS2) and the ITS II region (between the primers ITS3 and ITS4) had the highest resolution for identifying wood rotting fungi. To assess about the diversity of the *T*(m), intraspecific diversity of these DNA fragment sequences was evaluated using test strain sequences and data from the GenBank/EMBL/DDBJ biological database. The intraspecific diversity of *T*(m) was considered to be small because the nucleotide diversity of each fragment was small within the species.

Keywords Species identification · Melting temperature · Fungi · Real-time PCR · Nucleotide diversity

Introduction

Identification of fungal species, including wood rotting fungi, based on the morphology of fruiting bodies is difficult because time and environmental conditions change their morphology. Moreover, hyphal morphology and physiological features did not provide sufficient information to allow identification of fungal species. Tubes or dishes with fungal strains in them can be confused in the daily laboratory work. Identification of wood rotting fungi is important in the research of wood degradation and in the ongoing development of wood preservation. A correct, rapid, and convenient method to identify fungi is needed.

Recently, certain methods based on the information of biomolecules have been become popular for the identification of wood rotting fungi [1–8]. In particular, methods based on DNA nucleotide sequences are attractive because of their simplicity and accuracy [9–14]. The sequences used for fungal species identification and typing are ribosomal RNA genes (rDNAs), which contain three rDNA, the 18S, 28S, and 5.8S rDNA; inter transcribed spacer (ITS) regions; and a large intergenic spacer (IGS) region [15]. Sometimes another rDNA, the 5S, may be present within the IGS. The rDNA copy number varies widely; in most eukaryotes, it is between 30 and 30,000 copies [16] and the repeats are organized tandemly at one or more sites per haploid genome. The ITS region is located between the 18S and the 28S rDNA and consists of two spacers, the ITS I and the ITS II, and the 5.8S rDNA (Fig. 1). The spacers allow mutations and accumulate diversities of nucleotide sequences and length. Thus, the ITS region was employed

Part of this report was presented at the 65th annual meeting of the Japan Wood Research Society, Sapporo, March 2012.

S. Horisawa (✉)
Department of Environmental Systems Engineering, Faculty of Engineering, Kochi University of Technology, Kami-gun, Kochi 782-8502, Japan
e-mail: horisawa.sakae@kochi-tech.ac.jp

Y. Sakuma
Graduate School of Science and Engineering, Ehime University, Matsuyama, Ehime 790-8577, Japan

S. Doi
Graduate School of Life and Environmental Sciences, University of Tsukuba, Tsukuba, Ibaraki 305−8572, Japan

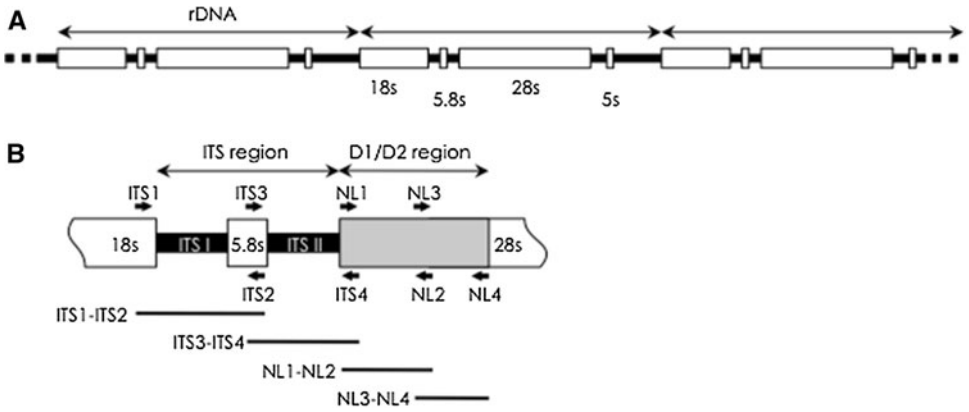

Fig. 1 Schematic diagram of the structure of fungal rDNA and the sites of the universal primers. **a** rDNA genes consisting of four genes, 18s rDNA, 5.8s rDNA, 28s rDNA, and 5s rDNA, are repeated. The *open wide bar* shows a coding region, and the *solid thin bar* shows a non-coding region. **b** The ITS region and the D1/D2 region. The ITS region consisted of the ITS I region, the ITS II region, and the 5.8s rDNA. *Short arrows* show the universal primers. *Bars* show the DNA fragments that are amplified by PCR using the universal primers

for the detection and identification of environmental fungi because of its high sensitivity and resolution [17–19]. The D1/D2 region, a part of the 28S rDNA has sufficient diversity to allow for characterizing species and was adopted for that purpose [20–22].

DNA sequencing has been the main method used to identify microbial species including fungi, but the process requires an enormous amount of time, cost, and effort in some cases, such as for the stock management of numerous fungal strains in a laboratory or for handling a huge group of samples in an environmental analysis. Therefore, a simpler and higher throughput method is needed. Species-specific primers are convenient for detecting and identifying species [19, 23–25], but the development of these primers take a long time because the primers should be designed for each species. The melting temperature [*T*(m)] of a DNA fragment represents a characteristic of its sequence, because it is affected by its length and nucleotide sequence. The *T*(m) is obtained by melting curve analysis, which is conducted after polymerase chain reaction (PCR) amplification by means of a real-time PCR. The melting curve allows the analysis of differences in the *T*(m) to <0.1 °C and detection of a single nucleotide polymorphism, and is applied to the genotyping of pathogenic microbes [26–29]. The use of SYBR® green-based *T*(m) analysis lowers the cost of the procedure [30]. However, there have been no reports on the use of *T*(m)s representing character of long nucleotide sequences to identify fungal species.

In the present study, we determined the *T*(m)s of each of four types of DNA fragments to identify 20 species of wood rotting fungi that often appear in buildings and wood exteriors. The nucleotide variety of the sequences encountered in this study was investigated using not only the sequence information of the tested fungi, but also gene information obtained from the GenBank/EMBL/DDBJ database to examine the intraspecies variety of *T*(m).

Materials and methods

Fungal strains and DNA extraction

Fifty-seven strains of the 20-fungal species used in this study are listed in Table 1. The DNA of each fungal strain was extracted by the modified benzyl chloride method [31] using the ISOPLANT II DNA extraction kit (Nippon Gene, Tokyo, Japan). The mycelia of the test strains were collected from their growing mycelial mat on potato dextrose agar (PDA) plates. Approximately, 0.1 g of mycelia was placed in a 2.0-ml microtube, to which 500 µl of TE buffer (10 mM Tris–HCl, 0.1 mM EDTA, pH 8.0) and 10 µl of mercaptoethanol was added. Sample mycelia were ground for 2 min with a 7-mm zirconia bead at a frequency of 25 Hz, using a TissueLyser mixer mill grinder (Qiagen, Inc., CA, USA). Then, the DNA was extracted from ground tissue using the ISOPLANT II. The extracted DNA was dissolved in TE buffer, and its concentration was measured using a Nano drop ND-1000 (Thermo Scientific, DE, USA).

Real-time PCR amplification and *T*(m) estimation by melting curve analysis

Four types of DNA fragments, the ITS I, the ITS II, and two parts of the D1/D2 region, were amplified using universal primers. The gene structure of rDNA including the ITS region, the D1/D2 region, and priming sites are shown in Fig. 1. Nucleotide sequences of the primers are shown in Table 2. In the present study, a DNA fragment between the

Table 1 Tested fungi

	Fungal strains tested	Type of wood decay[a]	Referenced sequences for ITS	Referenced sequences for D1/D2
Bjerkandera adusta	NBRC 4983, NBRC 5307, NBRC 104974, KUT 0804	WR	FJ810147, EU918694, AB096737, JF439464, AB567717, AF455468, HQ327995, AJ006672, AF455440, AY089741, JN198491, FJ608590, EF441742, HM164585, FJ228211	GQ47062, AB096738, FN298244, AF287848, AY858352
Coniophora puteana	NBRC 6275, fpri-M	BR	AM946631, AJ249502, AJ249503, AJ344109, GU187513, GU187521, AJ344110, AY736026, AY736023, AY736025, AY736020, AY736028, AY736027, AY736024, AY736021, GU187520, AY736022, EU722763, AY736019	AM946631, AJ583426, GU187578, GU187577, AF352039, AF098377
Daedalea dickinsii	NBRC4979, NBRC6487, NBRC30766, NBRC31163	WR	FJ810178, FJ481049, EU661878, FJ810145, FJ810167, FJ810173	EU024963, JF416685, AY858358
Fomitopsis palustris	NBRC 30339	BR	HM126460, EU024965, AB604156, DQ491404	AB604155, EU024964, JQ410896
Ganoderma gibbosum	KUT0805	WR	FJ582638, EU273513, EU273555, EU918695, EU273514, EU326219, EU326218, AY593854, AY593855, EU273557, AY593857, AY593856, FJ392286, JN008873, GU213473, GU213472, DQ425009, DQ424996, GU213474, AY884184	–
Ganoderma lucidum	GAL-M, NBRC 31863	WR	JN222421, EU021455, JN008871, JN222425, JN008870, FJ940919, JN008869, HQ235632, HQ235631, HQ235630, FJ379262, EU021456, GU213483, GU213479, GU213478, GU213484, GU213481, EU498091, GU213485, GU213487, GU213480, GU213477, GU213476, FJ501568, FJ501559, FJ501555, FJ501553, FJ501577, FJ501576, FJ501569, FJ501557, FJ501554, FJ379263, GU213471, EU520247, FJ379265, EF188279, EF188278, EF188277, HQ222603, EU520235	DQ208411, DQ208413
Gloeophyllum sepiarium	NBRC4944, NBRC6267	BR	AJ420946, AJ344141, AF527519, HM536091, AY089732, GU067756, GU067756, JN182924, AY497555, FJ903356, EU162055	AJ583432, AY333806, AY333805, AF393059
Gloeophyllum striatum	NBRC 6429, NBRC 30341, NBRC 6506	BR	HM536092	HM53606
Gloeophyllum trabeum	NBRC 6430, NBRC 6509	BR	AJ420949, JF682771, GQ337913, AJ420950, HM536093, HM536094, AY089733, AF423117, FJ789778	HM536067, EU232301, AY333804, AY333803, AF139948
Neolentinus lepideus	NBRC 6645, NBRC 8719, NBRC 30750	BR	GQ337914, EF524039, HM536098, FJ235147	–

Table 1 continued

	Fungal strains tested	Type of wood decay[a]	Referenced sequences for ITS	Referenced sequences for D1/D2
Pleurotus cystidiosus	NBRC30607	WR	DQ882570, DQ882572, FJ040175, AY315771, AY315776, AY315778, AY315767, AY265818, AY315774, AY315777, AY315770, AY315773, AY315769, EF514244, FJ608592, AB115041, EU424282, DQ882571, EU424280, DQ882573, DQ978222, AY315805, EU424278, AY315796, AY315804, AY315795, AY315797, AB115054, AY315792, AY315809, JF758877, AB115036	EU365637, EU365636, U04149, U04148, EU365639, EU365638
Pleurotus ostreatus	NBRC 6515, NBRC 30160, NBRC 33211	WR	AY540332, EU424300, EU520110, AY450345, EF514248, FJ501564, FJ501549, EU520108, EU520107, FJ501550, EF514242, EU622250, AY540325, EU622254, AY540324, FJ501552, JF758887, HM590443, DQ077884, AY368665, AY265839, GU722280, FN391585, AB115040, AY636055, AY540333, AY540322, EF514247, AY854077, AB115051, AY265831, AY265829	–
Pleurotus pulmonarius	NBRC 30791	WR	FJ379269, AY540328, FJ810164, AY696300, FJ379270, AY450349, GQ249869, GQ249877, AY540330, AY696298, AB115046, AY696299, JN043318, HM590446, HM590442, HM590441	EU365668, AY450349, AY524787, EU365666, PU04157, PU04153, PU04151, PU04145, PU04141, U04152, EU365669, EU365667, EU365660, JF736660
Schizophyllum commune	KUT 0503, NBRC 4928, NBRC 6502, NBRC 30496, NBRC 30749,	WR	JF439509, EU530002, EF155505, AF280758, AF280757, AF280756, AF280754, AF280753, AF280752, AF280750, AB428350, AB470852, AB369910, HQ684720, AB566277, AB369909, AF350925, EU520209, AF280759, FJ462753, GQ249871, AM269809, AF348142, HM595559, FJ372688, HM992521, GQ249870, AF280758, FJ372690, FJ372682, AJ537502, GQ254677, AJ537503, FJ372683, HQ327997, EU853847, AY949987, JF502460, FJ426395, HM775083, JN198386, HQ327996, AB470861, HQ327998	AB428351, AB363767, AB363768, AF261587, HM595605, AM269871, AJ406555, DQ071725, AF334751, FJ372712, FJ372705, GQ254661, AY858374, GQ241260, FJ471576, AB080723
Serpula lacrymans	fpri7906, fpri8015, fpri8113, fpri8209, fpri8601, fpri8603, fpri8604, fpri8701, fpri8804, fpri9302, fpri9401, NBRC 8697, NBRC 30955	BR	AM946630, AJ536025, AJ419908, AJ437601, AJ536022, AJ536023, AM946629, AJ419909	AM946629, AJ440941, AJ440940, AJ536023, AJ536022, AJ437601, GU187596, AJ536022, AJ536023, AJ440941
Stereum hirsutum	NBRC 6520	WR	AM269810, AY85406, DQ400105, DQ400106, DQ404322, DQ404323, EU673087, EU673088, EU673089, EU851110, EU851111, EU851113, FJ810129, FJ810141, FJ810144, FJ810148, FJ999712, FJ999713, FN539063	AY039334, AY039330, AF393078, AF506479, AM269874, AF385165, FJ471554, AY858376
Trametes cinnabarina	NBRC 8255	WR	DQ411525, AF363766, AF363765, AF363764, AF363757, AF363756	AY586703, HQ891294, AF261536, HQ891298, AF393074, AJ488128

Table 1 continued

	Fungal strains tested	Type of wood decay[a]	Referenced sequences for ITS	Referenced sequences for D1/D2
Trametes hirsuta	NBRC 4917, NBRC 4920, NBRC 6477, NBRC 7038	WR	HQ896244, JF308949, EF546237, FR686582, AF516556, JF439511, HQ891292, EF546240, HM004553, FJ550367, EU326211, EU273560, GQ280373, GQ280372, FJ462747, AF516563, HQ435856, HQ435867, HQ435855, HQ435843, HQ435841, HQ435860, HQ435848, HQ435857, HQ435840, JN182922, HQ435869, HQ435853, HQ435859, HQ435846, HQ248218, HQ435839	AY351923, AY351922, AJ488129
Trametes pubescens	NBRC 7892	WR	HQ435870, HQ435864, HQ435858, HQ435851, HQ435845, DQ925487, AY684173, EU153542	AY515341, AY855906
Trametes versicolor	NBRC 4937, NBRC 4940, NBRC 6481, NBRC 8754, NBRC 30388, NBRC 30340, KUT 0702, KUT 0705, KUT1002	WR	AY840580, AY840578, AY309015, AY840586, EF524040, EF546242, EU661891, AY309018, AY840583, GQ411515, FJ810179, JF439512, HQ172001, EF524042, AY840585, AY840584, AY309016, EF546241	HM595617, AY333793, DQ208417, DQ208416, AY684159, AF347107, AF139961, DQ208415, DQ208414

[a] WR and BR show white rot and brown rot, respectively

Table 2 List of universal primers used

Name of primes	Sequence (5′–3′)
ITS1	tccgtaggtgaacctgcgg
ITS2	gctgcgttcttcatcgatgc
ITS3	gcatcgatgaagaacgcagc
ITS4	tcctccgcttattgatatgc
NL1	gcatatcaataagcgg aggaaaag
NL2	ctctcttttcaaagttcttttcatct
NL3	agatgaaaagaactttga aaagagag
NL4	ggtccgtgtt tcaagacgg

primers is represented using the names of the two primers; for example, a fragment between primers ITS1 and ITS2, the ITS I, is presented as "ITS1–ITS2" and another fragment between the primers NL1 and NL2 is presented as "NL1–NL2". Real-time PCR was performed in a 20-μl reaction containing 1 ng template DNA, SYBR® Premix Ex Taq™ Perfect Real Time (Takara Bio, Inc., Shiga, Japan) and 200 μM of each forward and reverse primer. The following program was performed on the Applied Biosystems 7000 real-time PCR system (Applied Biosystems, CA, USA): an initial denaturization step at 95 °C for 5 min followed by 40 cycles of denaturization at 95 °C for 5 s, followed by annealing and extension at 60 °C for 41 s [19]. After that, a dissociation stage was added with a slow ramp to 95 °C. The real-time PCR and melting curve analyses were carried out in triple-replication using three reaction wells for each template DNA.

Sequence analysis

Four types of DNA fragment were amplified by PCR using the Takara Ex Taq™ (Takara Bio, Inc., Shiga, Japan). The mixture contained 10 ng of template DNA; each primer at a concentration of 0.5 pM; each dNTP at a concentration of 200 nM, 1.2 U/100 μl of DNA polymerase; and expand reaction buffer with 1.5 mM $MgCl_2$. PCR was performed with a GeneAmp 2720 thermal cycler (ABi, CA, USA) with the following parameters: an initial denaturization of 5 min at 95 °C, 25 cycles of 30 s at 95 °C for denaturization, 30 s at 56 °C for annealing, 60 s at 72 °C for extension, and a final extension of 7 min at 72 °C. All PCR products were stored at 4 °C until use. Aliquots of PCR products were checked by running them on 1.0 % agarose gel. The PCR products were cloned into a sequence vector using the pGEM T-vector system (Promega, WI, USA). A BigDye Terminator Cycle Sequencing Ready Reaction Kit (Applied Biosystems) was used to sequence the re-amplified fragments. The sequenced reactions were performed with a Prism 3100 genetic analyzer (Applied Biosystems). Sequences were compared with the compilation of 16S rDNA genes available in the GenBank/EMBL/DDBJ database. A BLAST search identified the first sequences retrieved.

Table 3 Melting temperature [*T*(m)] of DNA fragments to identify species of wood rot fungi, ITS1–ITS2, ITS3–ITS4, NL1–NL2, and NL3–NL4

	ITS1–ITS2	(SD)	ITS3–ITS4	(SD)	NL1–NL2	(SD)	NL3–NL4	(SD)
Bjerkandera adusta	86.5	(0.17)	85.9	(0.64)	85.8	(0.45)	87.0	(0.30)
Coniophora puteana	82.8	(0.00)	85.2	(0.00)	85.9	(0.00)	85.4	(0.28)
Daedalea dickinsii	84.7	(0.30)	83.8	(0.07)	85.2	(0.19)	86.8	(0.17)
Fomitopsis palustris	85.3	(–)	84.4	(–)	85.2	(–)	87.3	(–)
Ganoderma gibbosum	86.3	(–)	86.1	(–)	85.2	(–)	88.2	(–)
Ganoderma lucidum	86.7	(0.23)	86.2	(0.12)	85.2	(0.00)	88.0	(0.00)
Gloeophyllum sepiarium	84.6	(0.00)	84.2	(0.09)	85.1	(0.21)	87.1	(0.28)
Gloeophyllum striatum	84.3	(0.19)	84.0	(0.00)	85.2	(0.00)	86.9	(0.00)
Gloeophyllum trabeum	85.5	(0.14)	84.1	(0.00)	85.1	(0.21)	87.1	(0.21)
Lentinus lepideus	84.7	(0.23)	86.2	(0.28)	84.9	(0.23)	87.2	(0.28)
Pleurotus cystidiosus	84.2	(–)	83.3	(–)	85.1	(–)	86.5	(–)
Pleurotus ostreatus	83.4	(0.12)	84.3	(0.17)	85.0	(0.20)	85.4	(0.17)
Pleurotus pulmonarius	83.5	(0.00)	83.7	(0.14)	85.0	(0.28)	85.5	(0.00)
Pycnoporus cinnabarinus	87.6	(–)	86.3	(–)	85.8	(–)	88.6	(–)
Schizophyllum commune	83.0	(0.20)	85.6	(0.00)	85.3	(0.19)	87.7	(0.08)
Serpula lacrymans	84.4	(0.09)	84.4	(0.13)	86.1	(0.11)	86.6	(0.06)
Stereum hirsutum	85.1	(–)	86.3	(–)	85.4	(–)	88.5	(–)
Trametes hirsuta	86.8	(0.35)	85.5	(0.19)	85.6	(0.00)	88.0	(0.00)
Trametes pubescens	86.2	(–)	84.9	(–)	85.7	(–)	88.2	(–)
Trametes versicolor	86.3	(0.42)	84.9	(0.23)	85.6	(0.09)	88.1	(0.08)

SD in parentheses shows a standard deviation of *T*(m)

Calculation of nucleotide diversity (π)

Nucleotide sequences for the species tested were obtained from the GenBank/DDBJ/EMBL database to estimate intraspecific diversity (Table 1). The sequences that were analyzed and downloaded were aligned using ClustalX 2.0. [32] and then optimized manually. The DnaSP ver. 5.10. [33] was used to estimate the average nucleotide diversity π [34], which was computed from an aligned dataset for each kind of DNA fragments for each species.

Results

The *T*(m) of the rDNA fragments for fungal identification

T(m)s of the rDNA fragments for fungal identification were determined by melting curve analysis and intraspecific average, and standard diversities of the *T*(m)s were calculated (Table 3). The *T*(m) was measured at least thrice for each strain, and the results within each strain were in good agreement. The intraspecific diversity of *T*(m) varied according to species. The average of the *T*(m)s for each fragment of all species were 85.1, 85.0, 85.4, and 87.2 °C at ITS1–ITS2, ITS3–ITS4, NL1–NL2, and NL3–NL4, respectively. Concerning *Serpula lacrymans*, the standard deviations (SDs) of 13 strains, which were 0.09, 0.13, 0.11, and 0.06 in fragments ITS1–ITS2, ITS3–ITS4, NL1–NL2, and NL3–NL4, respectively, were very small; while the SDs of 9 *Trametes versicolor* strains, which were 0.42, 0.23, 0.09, and 0.08, respectively, were a little larger. The larger SDs were observed in *Bjerkandera adusta.* The measured *T*(m) of the strain of *B. adusta* NBRC 4983 differed from that of the other strains of *B. adusta*. The new average *T*(m)s from the other strains of *B. adusta* were 86.5 °C (± 0.17), 85.5 °C (± 0.12), 85.6 °C (± 0.25), and 86.3 °C (± 0.12) in fragments ITS1–ITS2, ITS3–ITS4, NL1–NL2, and NL3–NL4, respectively. A single strain was used in *Fomitopsis palustris*, *Ganoderma gibbosum*, *Pleurotus cystidiosus*, *Pycnoporus cinnabarinus*, *Stereum hirsutum*, and *Trametes pubescens*, and the SDs of these species were not obtained.

T(m) determination by the melting curve analysis in the present study had high reproducibility because it was almost not affected by quality and quantity of the template DNA solution. Multipeaks that indicate cross-contamination were not detected.

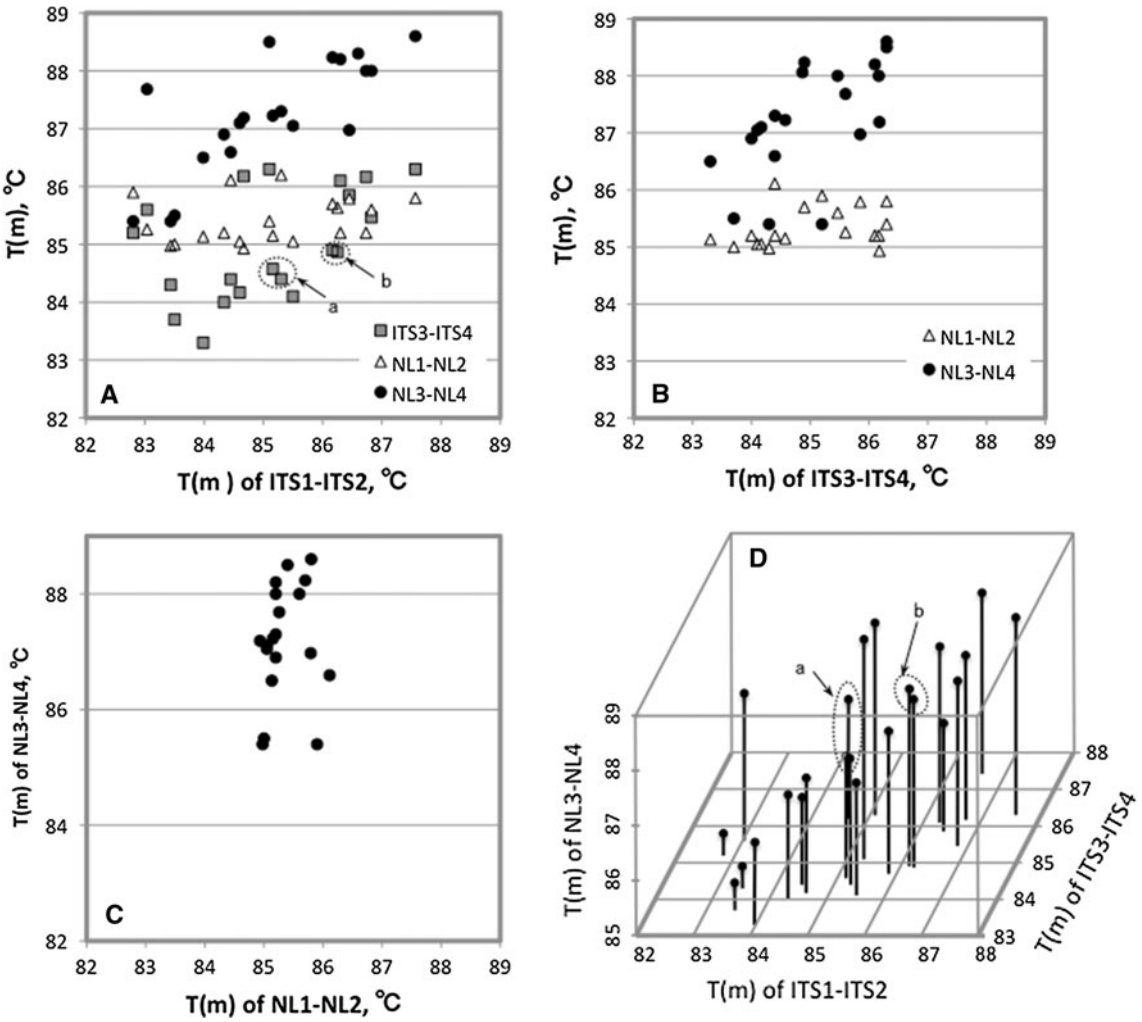

Fig. 2 Species identification by the combination of *T*(m)s from the four DNA fragments, ITS1–ITS2, ITS3–ITS4, NL1–NL2, and NL3–NL4. **A–C** The combination of two types of *T*(m). **D** The combination of three types of DNA fragments, ITS1–ITS2, ITS3–ITS4, and NL3–NL4. *Dotted circles* show examples of crowded plots; *a Fomitopsis palstris* and *Daedalea dickinsii*, *b Trametes pubescens* and *Trametes versicolor*

Species identification from the *T*(m) of the rDNA fragments

Fungal species discrimination using *T*(m) was examined for the 20 test species. Two types of *T*(m) were selected arbitrarily from the four, and one was plotted on the *X*-axis and the other on the *Y*-axis (Fig. 2A–C). The fact that the plots do not overlap implies that the combination of *T*(m)s has the ability to discriminate species. Sufficient diversity of *T*(m) to allow discrimination of the species was observed in fragments ITS1–ITS2, ITS3–ITS4, and NL3-NL4. The combination of ITS1–ITS2 and ITS3–ITS4 had higher resolution in most cases. The *T*(m)s of *Fomitopsis palustris* and *Daedalea dickinsii* were similar in this combination (Fig. 2A, a), as were those of *T. pubescens* and *T. versicolor* (Fig. 2A, b). For higher resolution, we examined the combination of three *T*(m)s for fragments ITS1–ITS2, ITS3–ITS4, and NL3–NL4 (Fig. 2D). The three-dimensional analysis was sufficient to discriminate those species.

Intraspecific diversity of nucleotide sequences

The four types of DNA fragments for each strain used in this study were determined and submitted to the DDBJ database. The accession numbers of the sequences determined in this study are AB592333–AB592336, AB733118–AB733170, AB733173–AB733301, AB733420–AB733431, and AB733644–AB733646 for the ITS region and AB592333, AB733172, AB733299–AB733348, and AB733411–AB733419 for the D1/D2 region. The average nucleotide diversity (π) of each DNA fragment for every species was calculated using the determined and downloaded sequences (Table 4). The π value exhibits the average number of

Table 4 Nucleotide diversity (π) of DNA fragments to identify species of wood rot fungi, ITS1–ITS2, ITS3–ITS4, NL1–NL2, and NL3–NL4

	ITS1–ITS2		ITS3–ITS4		NL1–NL2		NL3–NL4	
	π	n*	π	n*	π	n*	π	n*
Bjerkandera adusta	0.121	17 (4)	0.011	17 (4)	0.001	7 (4)	0.011	7 (4)
Coniophora puteana	0.003	21 (2)	0.004	21 (2)	0.001	8 (2)	0.001	8 (2)
Daedalea dickinsii	0.005	9 (3)	0.005	9 (3)	0	6 (3)	0	6 (3)
Fomitopsis palustris	0	5 (1)	0.002	5 (1)	0	3 (1)	0	3 (1)
Ganoderma gibbosum	0.004	14 (1)	0.005	14 (1)	–	1 (1)	–	1 (1)
Ganoderma lucidum	0.005	42 (2)	0.004	39 (2)	0	5 (2)	0.001	5 (2)
Gloeophyllum sepiarium	0.006	12 (2)	0.005	12 (2)	0	5 (1)	0.004	5 (1)
Gloeophyllum striatum	0.026	4 (3)	0.022	4 (3)	0.008	2 (1)	0.014	2 (1)
Gloeophyllum trabeum	0.004	11 (2)	0.001	11 (2)	0.002	7 (2)	0	7 (2)
Lentinus lepideus	0.044	5 (1)	0.018	5 (1)	0.004	3 (1)	0.021	3 (1)
Pleurotus cystidiosus	0.039	35 (1)	0.035	35 (1)	0.014	7 (1)	0.007	7 (1)
Pleurotus ostreatus	0.012	38 (3)	0.004	38 (3)	0.002	3 (3)	0.005	3 (3)
Pleurotus pulmonarius	0.001	17 (1)	0.002	17 (1)	0.008	14 (2)	0.001	14 (2)
Pycnoporus cinnabarinus	0.001	7 (1)	0.006	7 (1)	0.003	7 (1)	0.012	7 (1)
Schizophyllum commune	0.006	56 (5)	0.004	54 (5)	0.002	19 (6)	0.003	21 (6)
Serpula lacrymans	0.004	20 (12)	0.007	20 (12)	0	14 (7)	0	14 (7)
Stereum hirsutum	0.030	20 (1)	0.015	18 (1)	0.005	8 (1)	0.003	6 (1)
Trametes hirsuta	0.014	36 (4)	0.007	58 (4)	0.002	7 (4)	0.003	7 (4)
Trametes pubescens	0.019	9 (1)	0.002	8 (1)	0	3 (1)	0.005	3 (1)
Trametes versicolor	0.010	27 (9)	0.005	27 (9)	0.001	15 (6)	0.001	15 (6)

The numbers in parentheses are the number of sequences analyzed in the present study

* With n shows the number of sequences used in the analysis

nucleotide differences per site from two randomly selected sequences. The π values were small, <0.05 in all the ITS fragments except for the ITS of *B. adusta,* and close to 0.02 or less. The π of *B. adusta* in fragment ITS1–ITS2 was high, 0.121. To examine the cause, we checked the sequence data very carefully. The alignment data of fragment ITS1–ITS2 from the 17 sequences of *B. adusta* showed that only one sequence, AB733156 from *B. adusta* NBRC 4983, was very different from the others. The new alignment data eliminated the sequence of *B. adusta* NBRC 4983, which had a π value of 0.005, which was low compared to that of other species. Blast search showed that the whole region of ITS of *B. adusta* NBRC 4983 had a level of homology at 95 % with other ITS sequences of *B. adusta*, which was on a borderline between identification and error, and 99 % homology with *Bjerkandera fumosa* (AJ006673 and FJ903376). However, there was insufficient data on *B. fumosa* to evaluate whether NBRC 4983 was misidentified.

Discussion

The results showed that the *T*(m)s of fragments ITS1–ITS2, ITS3–ITS4, and NL3–NL4 have almost enough diversity to identify species. The length of the ITS and D1/D2 regions that can be used as probes for species identification is 650 bp each. If a DNA fragment becomes long, the *T*(m) will become high and the difference in diversity of the nucleotide sequences will become hard to be reflected. Therefore, these probes were divided into two fragments, respectively. The average length of the fragments ITS1–ITS2, ITS3–ITS4, NL1–NL2, and NL3–NL4 in all tested species were 278.7 (±21.8 SD) bp, 388.9 (±19.4) bp, 353.9 (±10.3) bp, and 307.1 (±15.7) bp, respectively. To identify species using the PCR-based fungal identification, the DNA fragment must be amplifiable using the universal primers that are applied to most organisms, even when no genetic information can be obtained. For these reasons, the four fragments used in this study are considered to be appropriate for the analysis using *T*(m).

The results showed that the combination of *T*(m)s of two types of fragment was sufficient to identify species and that the melting curve analysis is a simple but effective, low cost tool for identifying fungal species. As many strains of each species as possible need to be tested to obtain a more accurate diagnosis. However, it is difficult to both collect a large number of strains and precisely identify the species. We calculated the data of the nucleotide diversity using the data of nucleotide sequence in the gene database and estimated the accuracy and intraspecific diversity of

T(m) based on that calculation. The nucleotide diversities of the four types of DNA fragment were small in most of the species tested, and the diversity of the ITS region was larger than that of the D1/D2 region. It is easy to understand results because the ITS region is a non-coding spacer and the D1/D2 codes for the rRNA fragment. The intraspecies diversity of *B. adusta* is notable, because it reveals a problem of species diagnosis based on the nucleotide sequences. The case of *B. adusta* suggests that misidentification of species or the multi-genetic type included in the species leads to the estimation of a large *T*(m) and nucleotide diversity. In particular, having fewer samples may result in larger diversity. Therefore, the accumulation of accurate nucleotide information about fungi is required for improvement of the species identification method based on the DNA sequences. The 20 species in the present study were mainly selected as the fungi that often attack wooden house and construction. For utilizing *T*(m) of DNA as one of identification tools, a *T*(m) database also from many other species has to be established. Incorrect identification will be avoided using *T*(m) in conjunction with information on the fungal growing environment, decay type, mycelial morphology, etc. For example, *F. palustris* and *D. dickinsii*, those were not discriminated by two-dimensional *T*(m)s, could be distinguished using *T*(m)s together with their decay type (Table 1). However, it was impossible to discriminate of *Trametes hirsuta* and *T. pubescens* even using decay type. A dendrogram based on the ITS sequences of *T. hirsuta* and *T. pubescens* showed that some sequences of both species fell into the same cluster (data not shown). Therefore, re-examining classification of DNA sequences referenced is required to enhance the reliability of this typing method. The *T*(m)s will be a useful laboratory tool for the stock management of fungal strains because *T*(m) measurement is simpler and less cost with sequencing which is a conventional practice.

Acknowledgments We would like to thank Mr. Kensuke Hanata of the Akita Wood Technology Transfer Foundation for useful suggestions and Mr. Masato Maeda and Mr. Kodai Hamaguchi of Kochi University of Technology for their technical assistance.

References

1. Palfreyman JW, Vigrow A, Button D, Herarty B, King B (1991) The use of molecular methods to identify wood decay organisms. 1. The electrophoretic analysis of *Serpula lacrymans*. Wood Prot 1:5–22
2. Palfreyman J, Vigrow A (1994) Molecular analysis of certain isolates of *Serpula lacrymans*. FEMS Microbiol Lett 117:281–286
3. Clausen C (1994) Dyed particle capture immunoassay for detection of incipient brown-rot decay. J Immunoass 15:305–316
4. Palfreyman JW, Bruce A, Button D, Glanct H, Vigrow A, King B (2001) Immunological method for the detection and characterization of wood decay basidiomycetes. Int Biodeterior Biodegrad 48:74–78
5. Clausen CA, Green F, Highley TL (1991) Early detection of brown-rot decay in southern yellow pine using immunodiagnostic procedures. Wood Sci Technol 26:1–8
6. Jellison J, Goodell B (1988) Immunological detection of decay in wood. Wood Sci Tech 22:293–297
7. Naumann A, Navarro-González M, Peddireddi S, Kües U, Polle A (2005) Fourier transformation infrared microscopy and imaging: detection of fungi in wood. Fungal Genet Biol 42:829–835
8. Erukhimovitch V, Pavlov V, Talyshinsky M, Souprun Y, Huleihel M (2005) FTIR microscopy as a method for identification of bacterial and fungal infections. J Pharm Biomed Anal 37:1105–1108
9. Horisawa S, Sakuma Y, Takata K, Doi S (2004) Identification of intra- and inter-species of the dry rot fungus *Serpula lacrymans* by PCR-RFLP and RAPD analysis. J Wood Sci 50:427-432
10. Terashima K, Matsumoto T, Hasece K, Fukumasa-Nakai Y (2002) Genetic diversity and strain-typing in cultivated strains of *Lentinula edodes* (the shiitake mushroom) in Japan by AFLP analysis. Mycol Res 106:34–39
11. Majer D, Mithen R, Lewis BG, Vos P, Oliver RP (1996) The use of AFLP fingerprinting for the detection of genetic variation in fungi. Mycol Res 100:1107–1111
12. Barry T, Colleran G, Glennon M, Dunican LK, Gannon F (1991) The 16s/23s ribosomal spacer region as a target for DNA probes to identify eubacteria. PCR Methods Appl 1:51–56
13. Tooley PW, Goley ED, Carras MM, Frederick RD, Kuldau GA (2001) Characterization of *Claviceps* species pathogenic on sorghum by sequence analysis of the β-tubulin gene intron 3 region and EF-1 α gene intron 4. Mycologia 93:541–551
14. Roux J, Steenkamp ET, Marasas WFO, Wingfield MJ, Wingfield BD (2001) Characterization of *Fusarium graminearum* from Acacia and Eucalyptus using β-tubulin and histone gene sequences. Mycologia 93:704–711
15. Long EO, Dawid IB (1980) Repeated genes in eukaryotes. Annu Rev Biochem 49:727–764
16. Prokopowich CD, Gregory TR, Crease TJ (2003) The correlation between rDNA copy number and genome size in eukaryotes. Genome 46:48–50
17. Guarro J, Gené J, Stchigel AM (1999) Developments in fungal taxonomy. Clin Microbiol Rev 12:454–500
18. Iwen PC, Hinrichs SH, Rupp ME (2002) Utilization of the internal transcribed spacer regions as molecular targets to detect and identify human fungal pathogens. Med Mycol 40:87–109
19. Horisawa S, Sakuma Y, Doi S (2009) Qualitative and quantitative PCR methods using species-specific primer for detection and identification of wood rot fungi. J Wood Sci 55:113–138
20. Fell JW, Boekhout T, Fonseca A, Scorzetti G, Statzell-Tallman A (2000) Biodiversity and systematics of basidiomycetous yeasts as determined by large-subunit rDNA D1/D2 domain sequence analysis. Int J Syst Evol Microbiol 50:1351–1371
21. Kurtzman CP, Robnett CJ (1998) Identification and phylogeny of ascomycetous yeasts from analysis of nuclear large subunit (26S) ribosomal DNA partial sequences. Antonie Van Leeuwenhoek 73:331–371
22. Scorzetti G, Fell JW, Fonseca A, Statzell-Tallman A (2002) Systematics of basidiomycetous yeasts: a comparison of large subunit D1/D2 and internal transcribed spacer rDNA regions. FEMS Yeast Res 2:495–517
23. Suhara H, Maekawa N, Kubahashi T, Kondo R (2005) Specific detection of a basidiomycete, *Phlebia brevispora* associated with butt rot of *Chamaecyparis obtusa*, by PCR-based analysis. J Wood Sci 51:83–88
24. Schmidt O, Moreth U (1998) Genetic studies on house rot fungi and a rapid diagnosis. Holz Roh Werkst 56:421–425

25. Schmidt O, Moreth U (2000) Species-specific PCR primers in the rDNA-ITS region as a diagnostic tool for *Serpula lacrymans*. Mycol Res 104:69–72
26. Malentacchi F, Forni G, Vinci S, Orlando C (2009) Quantitative evaluation of DNA methylation by optimization of a differential-high resolution melt analysis protocol. Nucleic Acids Res 37:e86
27. Stephens AJ, Inman-Bamber J, Giffard PM, Huygens F (2008) High-resolution melting analysis of the spa repeat region of Staphylococcus aureus. Clin Chem 54:432–436
28. Merchant-Patel S, Blackhall PJ, Templeton J, Price EP, Tong SYC, Huygens F, Giffard PM (2010) *Campylobacter jejuni* and *Campylobacter coli* genotyping by high-resolution melting analysis of a flaA fragment. Appl Environ Microbiol 76:493–499
29. Anuj SN, Whiley DM, Kidd TJ, Ramsay KA, Bell SC, Syrmis MW, Grimwood K, Wainwright CE, Nissen MD, Sloots TP (2011) Rapid single-nucleotide polymorphism-based identification of clonal *Pseudomonas aeruginosa* isolates from patients with cystic fibrosis by the use of real-time PCR and high-resolution melting curve analysis. Clin Microbiol Infect 17:1403–1408
30. Zipper H, Brunner H, Bernhagen J, Vitzthum F (2004) Investigations on DNA intercalation and surface binding by SYBR Green I, its structure determination and methodological implications. Nucleic Acids Res 32:e103
31. Zhu H, Qu F, Zhu LH (1993) Isolation of genomic DNAs from plants, fungi and bacteria using benzyl chloride. Nucleic Acids Res 21:5279–5280
32. Larkin MA, Blackshields G, Brown NP, Chenna R, McGettigan PA, McWilliam H, Valentin F, Wallace IM, Wilm A, Lopez R, Thompson JD, Gibson TJ, Higgins DG (2007) Clustal W and Clustal X version 2.0. Bioinformatics 23:2947–2948
33. Rozas J, Sanchez-DelBarrio JC, Messeguer X, Rozas R (2003) DnaSP, DNA polymorphism analyses by the coalescent and other methods. Bioinformatics 19:2496–2497
34. Nei M (1987) Molecular Evolutionary Genetics. Columbia University Press, New York, p 257